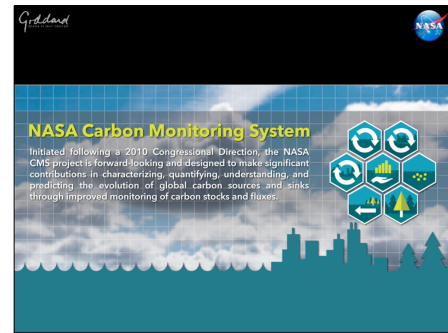




Welcome

Remote Sensing Applications for Wetland Inventories Workshop help at the Society of Wetland Scientists Meeting in San Juan, Puerto Rico on June 8th, 2017.



NASA CMS Introduction

NASA Carbon Monitoring System project is a congressional directive that is forward-looking and designed to make significant contributions in characterizing, quantifying, understanding, and predicting the evolution of global carbon sources and sinks through improved monitoring.

For more information about the NASA program, please visit the website at carbon.nasa.gov

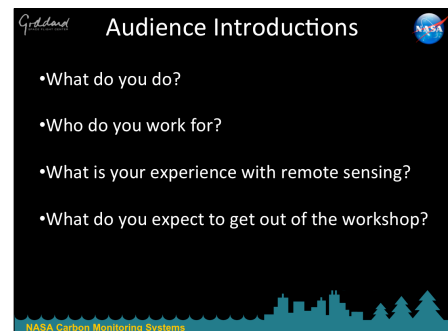


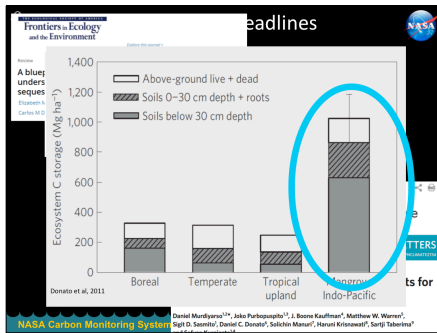
Speaker Introduction

Lola Fatoyinbo is a Research Scientist at NASA Goddard Space Flight Center, just outside Washington, D.C. There, she works on new methods to measure three dimensional forest structure from space. Her efforts have led to some of the first country-based mangrove biomass estimates for Africa.

Carl Trettin is a Research Scientist for the USDA Forest Service, based out of the Southeast Research Center in Cordesville, SC. He is a long-time soil biogeochemist and is working on coastal wetland carbon dynamics with the SWAMP program, USAID, and NASA.

David Lagomasino is an Assistant Research Professor at the University of Maryland. He works on coastal ecosystem vulnerability and resiliency. Using a multi-sensor approach to measure structural and functional components of wetlands.





Mangrove Blue Carbon Headlines

Blue carbon has been making headlines in recent years. This heightened sensitivity to mangroves, marshes, and seagrasses is a result of the ability of each of the ecosystems to capture organic matter and to hold onto it for a long time. Because of blue carbon capabilities, crediting programs have begun to incorporate wetlands into the carbon accounting. Wetlands will be featured in the upcoming State of the Carbon Cycle Report, and there are several mangrove forest projects that are underway to be certified by the Verified Carbon Standards program. This growth and excitement of blue carbon ecosystems is great. But we must also be cautious to how blue carbon is being estimated and reported. Today, we will discuss the application of remote sensing techniques that will help to provide an unbiased sampling protocol to improve mangrove carbon accounting.

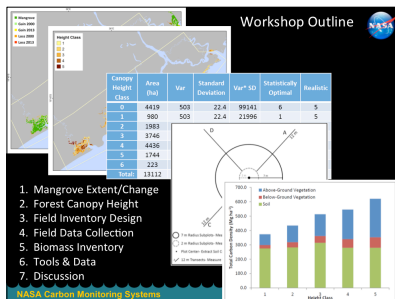
Workshop Objectives

- 1. Familiarize group with recent remote sensing applications in mangrove forests:** land cover, change and 3D height maps using multi-sensor data fusion (Polarimetric InSAR, Lidar, passive optical).
- 2. Examine remote sensing based forest inventory decision support tools:** collection of statistically representative samples of above and belowground carbon stocks in mangroves.

NASA Carbon Monitoring Systems

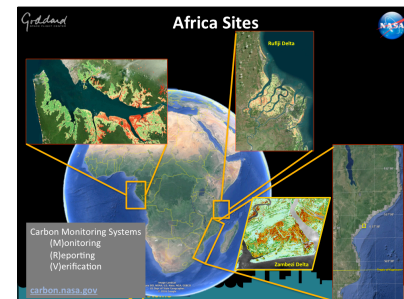
Workshop Objectives

In this workshop we will familiarize you with recent remote sensing applications in mangrove forests. This will include land cover and land cover change mapping, and three-dimensional forest structure. In addition, we will review how we can use that remote sensing data to create a forest inventory with decision support tools with the ultimate goal of providing unbiased estimates of mangrove carbon.



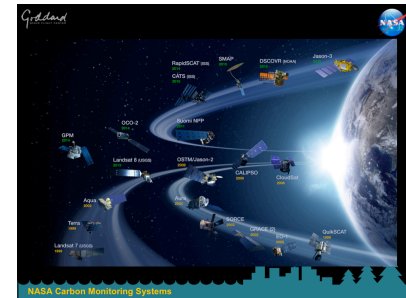
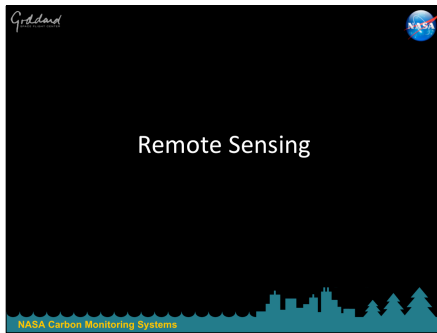
Outline of Workshop

In the workshop, we will briefly cover the methodology to generate mangrove extent and change and three-dimensional canopy height maps. Afterwards, we will explain how we can use those datasets to create a field inventory design and standardized field sampling protocols. Combining the remote sensing datasets with the field inventory, we will then illustrate how to estimate mangrove carbon stocks. Lastly, we will provide you with a list of tools and available (or soon to be available) datasets that can be used to implement this approach



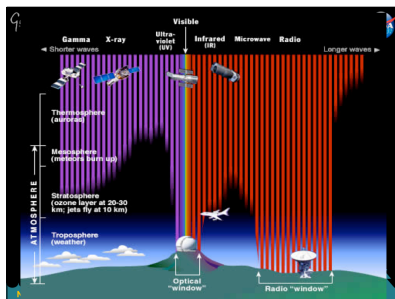
Our Study Sites

This workshop will pull data from various studies that our group has participated in. A subset of those studies come directly from a NASA Carbon Monitoring Systems project that our team is working on to improve the monitoring, reporting, and verification (MRV) of carbon for mangrove ecosystems in Africa: Mozambique, Tanzania, and Gabon with field measurements in the Zambezi Delta, Rufiji Delta and Gabon Estuary.



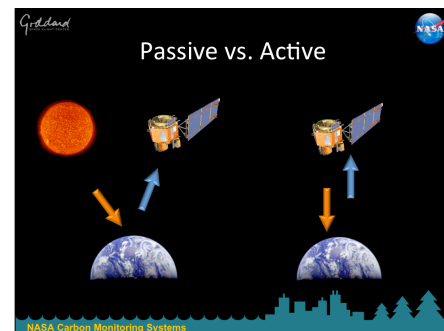
NASA Earth Observing Satellites

NASA's Earth Observing System is a coordinated series of polar-orbiting satellites that monitor the land surface, biosphere, solid Earth, atmosphere, and oceans for long-term global observations. We will focus on the satellites that provide information on the Earth's biosphere.



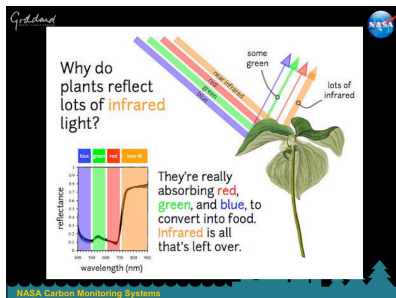
Energy and the Atmosphere

The incoming electromagnetic energy from the sun interacts with different gases and particles in our atmosphere. During this process, most of the energy is absorbed before it even reaches the surface of the Earth. The energy that does reach, is then reflected upwards and can be measured by sensors in space. There are two atmospheric "windows" that allow for the energy to pass through; the optical and radio window.



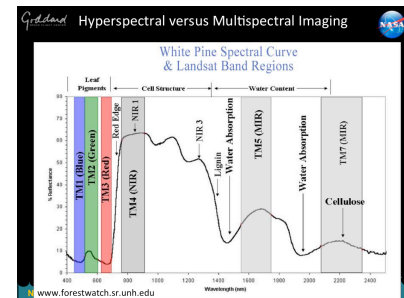
Passive vs Active

Passive sensors measure the solar energy that is reflected off the Earth's surface. Active sensors emit and measure a discrete energy pulse that reflects off the surface.



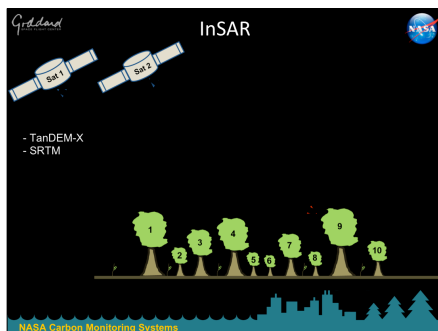
Vegetation Response

Energy within the optical “window” interacts with the different surfaces of the Earth. Different surfaces, including vegetation, absorb and reflect different portions of the EM spectrum. For plants, most energy is absorbed in the red and blue wavelength while most of the energy is reflected back in the Near-Infrared (NIR).



Hyperspectral versus Multispectral

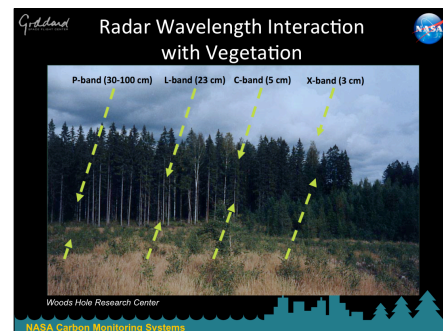
Optical sensors onboard Landsat satellites (e.g., Thematic Mapper, Enhanced Thematic Mapper Plus, Optical Land Imager) measure reflected energy from the Earth at targeted wavelengths in the blue, green, red, NIR, and Shortwave Infrared (SWIR).



Radar Background

Sensors similar to those on Landsat are called passive sensors. This means the source of energy being measured comes from the sun, and reflected off the Earth's surface. Sensors, like Synthetic Aperture Radar (SAR), are called active sensors because they emit the energy pulse that reflects off the land surface that is then measured by the same sensor.

Here is a schematic of how InSAR works, particularly in the case for SRTM (Shuttle Radar Topography Mission) and TanDEM-X. First, a radio pulse is emitted from one of the satellites. That pulse then interacts with the surface of the Earth, and the reflected signals are then returned whereby both sensors measure the returned pulse.



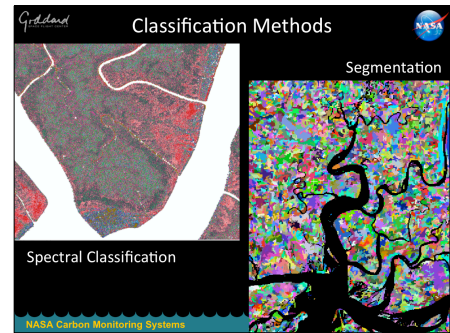
Radar Wavelengths:

The wavelength of the radar sensor interacts differently with the forest canopy. The longer the wavelength, the greater the sensitivity to the vertical structure of the vegetation. X-band wavelengths are shorter and interact with the top portion of the canopy. C-band wavelengths provides information about the top and mid-portion of the canopy. L-Band wavelengths interacts with most portions of the canopy including the ground, depending on the density of the vegetation.*

* X-band Satellites: TerraSAR-X, TanDEM-X, Cosmo-SkyMed

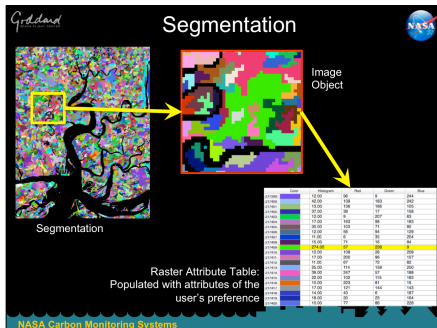
* C-band Satellites: Radarsat 1, Radarsat 2, Envisat, Sentinel 1

* L-band Satellites: ALOS-1, ALOS-2



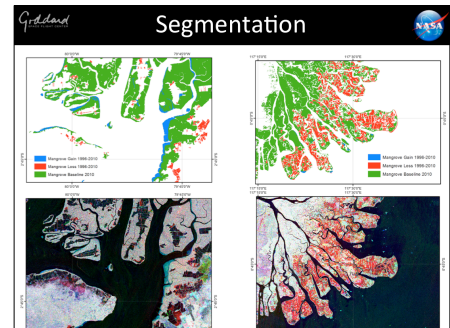
Classification Methods

Land cover classification analyzes the similarities in features using variety of land surface parameters. Traditionally, optical information from several bands are used in unsupervised and supervised classification schemes. More recently, additional band ratios, principal components analyses, and segmentations have been added to the schemes. Also information from different sensors provides an added layer of discrimination.



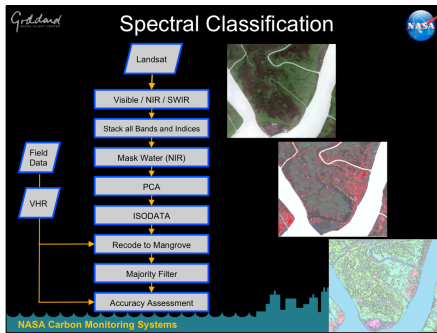
Segmentation

Segmentation is an approach to classify an image by extracting features based on objects. An image segmentation process creates these features where pixels close to each other and having similar spectral characteristics are grouped together into a segment. Afterwards, these segments can be grouped based on shapes, spectra, and spatial characteristics. Further, the objects can then be grouped into classes that are representative of real-world features.



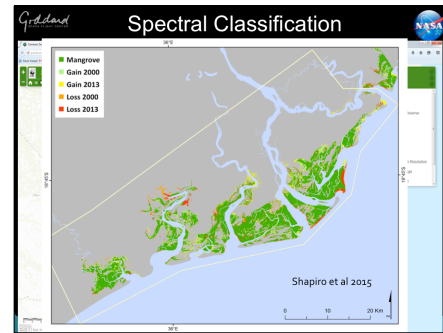
Segmentation Results

Here is an example of the results from a segmentation approach for classifying mangrove land cover using ALOS global mosaics. (Thomas et al, accepted)



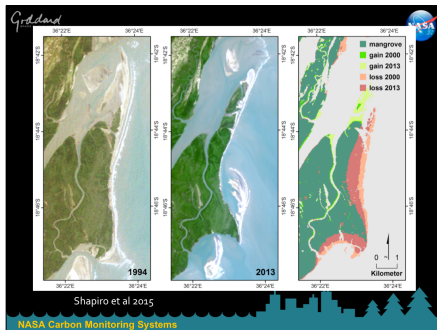
Spectra-Based Classification

Optical based classification methods start with stacking all the bands from one particular sensors (e.g., Landsat). Band rations such as Normalized Difference Vegetation Index, and Enhance Vegetation Index) are calculated from the original bands and added to the band stack. Water and/or elevation masks generated from set thresholds are used to remove unwanted areas. A principal component analysis (PCA) can then be run and stacked before running the ISODATA (or similar) algorithm. Afterwards, classes are recoded to mangrove land cover and a final accuracy assessment is used to determine the accuracy of the map.



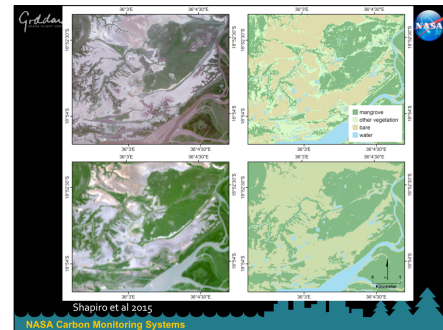
Land Cover Change in the Zambezi

Similar approaches have been applied to recent land cover mapping for the Zambezi Delta (Shapiro et al, 2015). The land cover classification was completed for 3 different time periods, 1994, 2000, and 2013. The difference between the various mangrove extent maps shows the areas of loss and gain over the 20 year period. Land cover change maps are available for the Zambezi are available at WWF. A link is available on our website through the data portal. (Shapiro et al, 2015)



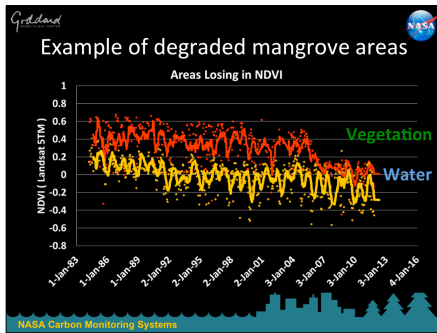
Land Cover Change Zambezi (Zoom)

Here we see a closer view of mangrove gains and losses in a region of the Zambezi Delta. Erosion and loss is highest along the seaward edge, while mangrove growth occurs around mud banks and spits. (Shapiro et al, 2015)



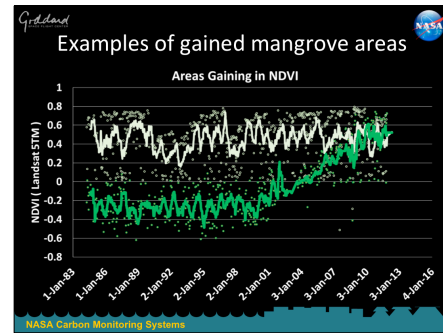
Land Cover Classification: VHR versus Landsat

Here we see the differences in detail between Landsat 30 m with a spatial resolution and very-high resolution data from WorldView 2 with a spatial resolution of ~2 m. (Shapiro et al, 2015)



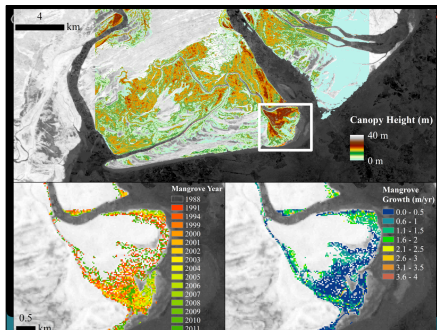
NDVI Mangrove Degradation

Mangrove forests can have a wide range of spectral variability depending on the time of year and inundation conditions. However, if we look at the long-term record we can deduce major changes/shifts in ecosystem structure. By using the Landsat image archive, we can use the “best” vegetation pixel value from every image to construct a long-term record of variability in forest cover. Here are two examples of degradation in mangrove forests. The data in red shows a rapid shift between mangrove forest (vegetation) to open/muddy water. The data in orange represents a more gradual mangrove degradation indicated by the linear negative slope over time.



NDVI Mangrove Regeneration

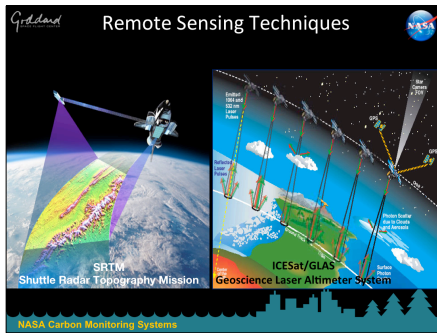
Similarly, we can also monitor mangrove regeneration and reforestation over time. The data in green show a shift in NDVI values from water (~0) to vegetation (~0.3). This is the gaining of new forested land from pioneering mangrove species. The data in white represents the forest response to weather anomalies (i.e., tropical storms, freeze events). The large oscillations are driven by the resilience of the forest. Combining the records together, we can begin to model the vulnerability and resiliency of different mangrove types.



Mangrove Loss/Gain Age

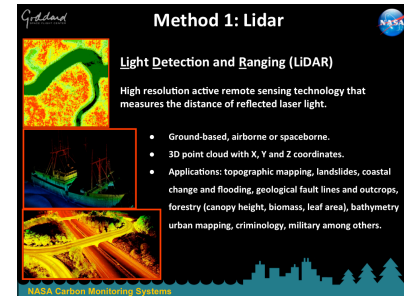
Using the long-term record, we can begin to estimate the age of the mangrove forest and the age of mangrove loss, particularly for those areas that show rapid changes. Combining those age relationships with canopy height data, derived from other data sources (next section) we can use a space-for-time approach to estimate the rate at which mangrove forests can grow vertically. (Lagomasino et al, in prep)





Remote Sensing Techniques:

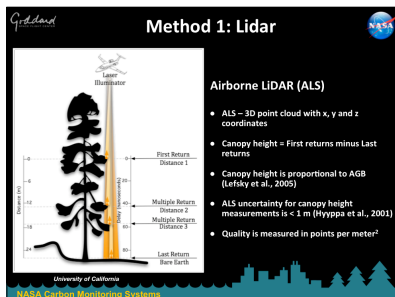
LiDAR - Light Detection and Ranging
 SAR - Synthetic Aperture Radar
 InSAR - Interferometric Synthetic Aperture Radar
 Very High Resolution (VHR) Stereo Photogrammetry



Lidar Background

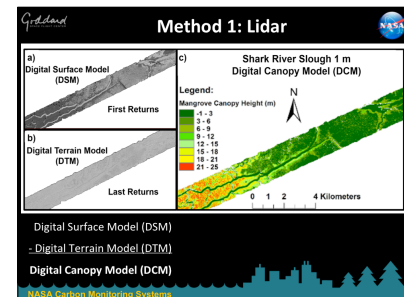
Some of the remote sensing techniques that we use include LiDAR. Lidar is the "gold-standard" for measuring forest structure parameters. Lidar stands for Light Detection and Ranging, and it measures the travel time of an emitted and reflected laser pulse. Lidar measurements can be collected from the ground, from the air, and from space. The resulting data provides information in three-dimensional space of measured objects. Lidar techniques have a wide range of applications. What will discuss in this workshop are applications for forestry. Particularly, forest canopy height.

30



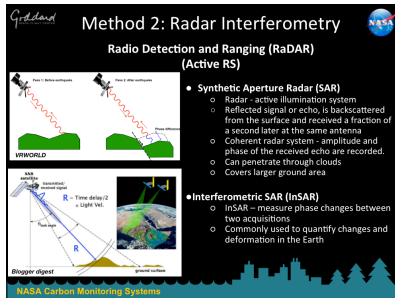
Airborne Lidar Background

Airborne Lidar, is flown on low-level aircrafts to measure the forest structure. Individual flight paths usually cover a swath of a few hundred meters. Therefore, measurements can be collected in strategic areas or collected wall-to-wall for maximum coverage. The time it takes for the laser pulse to be emitted and measured provides details of the canopy structure. Last returns, or the longest return time, represent the bare ground and are used to create Digital Terrain Models (DTMs), while the first returns, usually represent the top of the forest canopy and are used to create Digital Surface Models (DSMs).



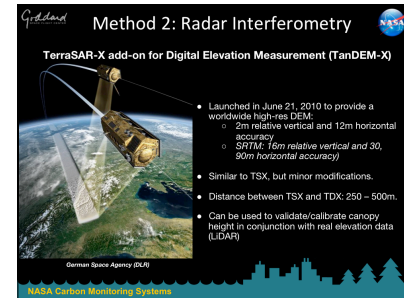
Digital Canopy Height (DCM) or Canopy Height Model (CHM)

Here we show a some examples of first returns and last returns from airborne lidar data. The Digital Surface Model (DSM, first returns) can be subtracted by the Digital Terrain Model (DTM, last return). The difference between the two datasets is the Digital Canopy Model, or Canopy Height Model (DCM or CHM). The height of the forest canopy provides important information for estimating the volume of biomass in the forest.



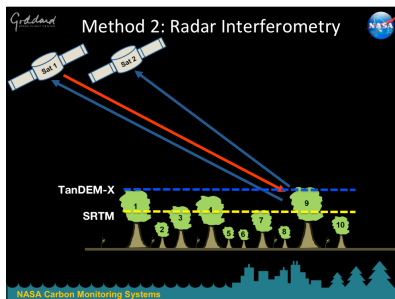
Radar Background

Radio Detection and Ranging (RaDAR) is similar to that of lidar but measures the return time of a radio wave instead of a green or NIR pulse. When the radio pulse interacts with the surface, it provides two parameters; amplitude and phase. Interferometric SAR (InSAR) is analogous with stereophotogrammetry for optical sensors. With InSAR, a radio pulse is emitted from one satellite, and measured at two different sensors with a set distance between them (baseline). Traditional InSAR is used to measure deformation features on the earth and changes in water levels. This can be done by using the differences in backscatter from repeat passes of the radar that could be a few days apart. The time delay can cause temporal decorrelation which inhibits the use on land surface like forests. However, bi-static measurements, or two measurements collected at the same time, can provide three-dimensional details of forest structure without the issues of temporal decorrelation.



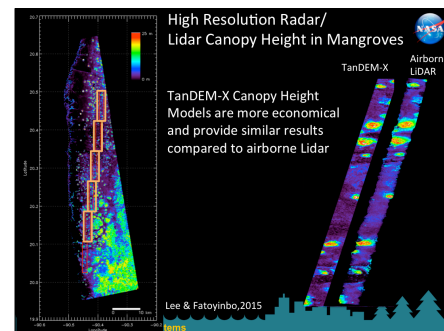
Radar InSAR

TanDEM-X, is a relatively recent satellite mission lead by the German Space Agency (DLR) that collects data from two satellites that fly in close formation. The satellite launched in 2010 with the goal of mapping a new global DEM. The two satellites are near-identical and fly at a distance of 250-500 m from each other. The near-instantaneous measurements do not have issues with temporal decorrelation and can be used to estimate canopy height. The data from TanDEM-X is not free, but at the cost between \$100 per scene and \$1000 per scene, the data is at a significantly lower cost than that of a similar acquisition with airborne lidar.



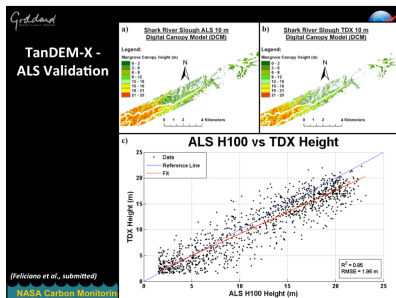
InSAR Schematic

Here is a schematic of how InSAR works, particularly in the case for SRTM (Shuttle Radar Topography Mission) and TanDEM-X. First, a radio pulse is emitted from one of the satellites. That pulse then interacts with the surface of the Earth, and the reflected signals are then returned whereby both sensors measure the returned pulse.



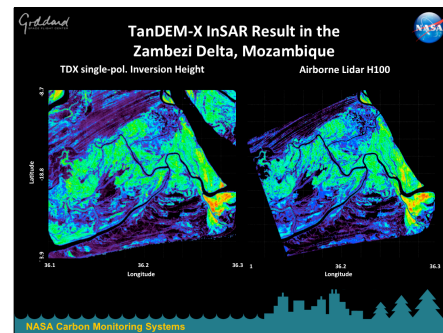
TanDEM-X Canopy Height

Here is an example of a TanDEM-X mangrove canopy height model for an area around Celestun, Mexico (Left). In the middle are 2 TanDEM-X scenes and in red outline you can see the airborne Lidar tracks highlighting how little data is acquired per lidar flight. On the right you will see a comparison between two overlapping areas of TanDEM-X and airborne lidar. The results area comparable, but one flight line of the lidar is a small percentage (orange boxes on left image) of the full coverage of the TanDEM-X image. (Lee and Fatoyinbo, 2015)



TanDEM-X versus Lidar (Everglades)

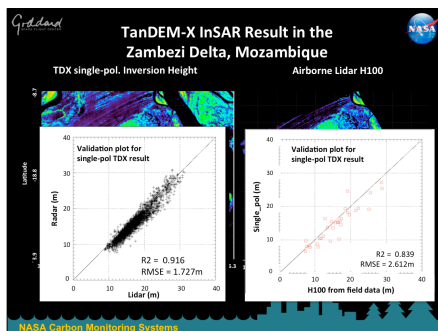
We have compared the canopy height estimates measured from TanDEM-X with those measured from airborne lidar in the mangrove forests of Everglades National Park. The top two images show overlapping digital canopy models for lidar (left) and TanDEM-X (right). The large chart on the bottom shows the pixel-by-pixel comparison between the lidar and TanDEM-X canopy height models. (Feliciano et al, submitted)



TanDEM-X versus Lidar (Zambezi)

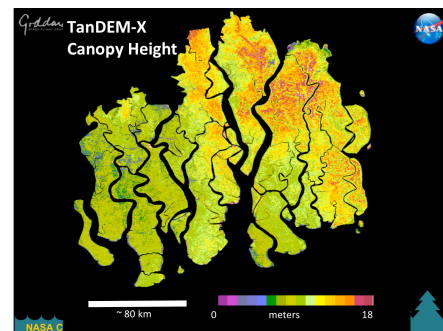
Here is another comparison between TanDEM-X (left) and airborne lidar (right) for an area of the Zambezi Delta. In this case airborne lidar was flown wall-to-wall over the region to provide a more continuous map.

37



TanDEM-X versus Lidar (Zambezi)

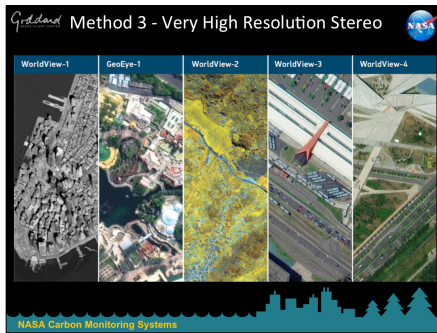
The validation between TanDEM-X pixels and airborne lidar pixels are shown on the left, resulting in a RMSE of 1.7 m. At this site, we also collected field data, and the comparison between field-measured heights and TanDEM-X are on the right.



Regional Canopy and Biomass Height Maps

TanDEM-X canopy height models from multiple acquisitions can then be mosaicked to provide regional, and country-wide estimates of mangrove canopy height. Here is an example of mangrove canopy height in the Sundarbans (Bangladesh). This is the largest continuous mangrove forest in the world.

Through our projects, we are mapping mangrove extent and canopy height for Mozambique, Tanzania, and Gabon.



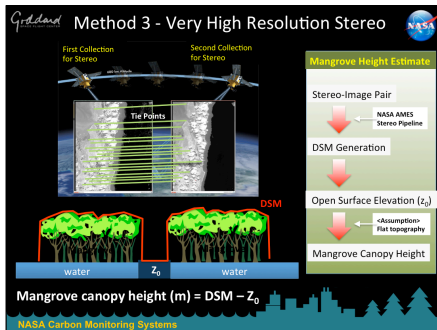
Very High Resolution Stereo

The last method that we will review in this workshop is very-high resolution stereo. Some commercial sensors, like those from Digital Globe, provide multispectral and panchromatic imager at spatial resolutions of ~2 m to less than 1 m, respectively.



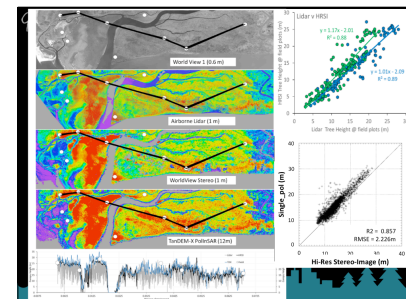
Digital Globe Satellites

Digital Globe has a number of satellites in orbit. The WorldView satellite series are four of those satellites. The figures here show the capabilities of each of the satellites along with different collection scenarios. In particular, we want to focus on the in-track stereo collection scenario.



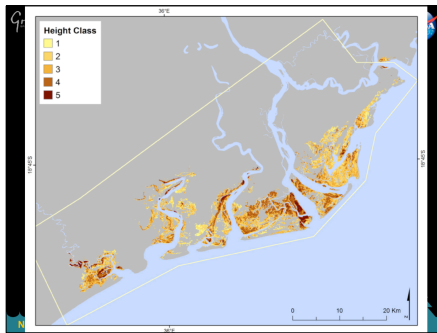
Satellite Stereo Photogrammetry

Here is a schematic of the stereo data technique. This is not a new technique, as stereo-photogrammetry has been around for a long time. But thanks to new legislation that went into effect a few years ago, we now have access to the entire archive of high resolution imagery collected by the National Geospatial Intelligence Agency, including thousands of stereo-pairs that allow us to generate high resolution digital elevation models. NASA Ames has developed the Ames Stereopipeline, software to process stereo satellite imagery, that is openly available and results in ~1m resolution digital surface models that are tied to reference elevations. After this step, we identify areas of bare ground to determine its elevation. Subtracting the ground elevation from the digital surface model generates the canopy height model. (Lagomasino et al, 2015; Lagomasino et al, 2016)



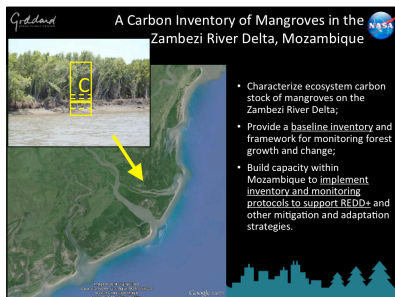
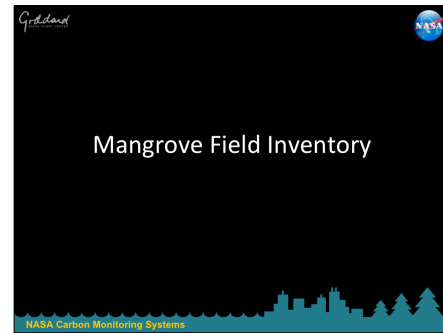
Canopy Height Model Comparison

Here is a five panel figure (left) showing the original panchromatic WorldView2 image over the Zamebzi, followed by three canopy height models derived from airborne lidar, WorldView stereo, and TanDEM-X. The last panel shows the canopy height comparison between each of the models along the black transect noted in the images. White circles are the locations of field sites and their measured forest heights are also noted. The comparisons graphs on the right show the validation between the WorldView stereo canopy height models and airborne lidar (top), and a similar graph comparing the stereo model with the TanDEM-X model.





Canopy Height Distribution

Using the canopy height information from any of those sources, we can derive the canopy height distribution for our region of interest. What this does is provide a new layer of data to improve our sampling protocols. In this case, we can use the height information from these models to stratify field inventories.



The field inventory of mangrove carbon stocks was supported by the U.S. Agency for International Development, and it was implemented in collaboration between the USDA Forest Service, Universidade Eduardo Mondlane, and World Wildlife Fund – Mozambique. Details of the project design and results are available in Stringer et al. (2015). The distribution of mangroves within the Zambezi River Delta is available in Shapiro et al. (2015).





Assessment Design – The Critical Step

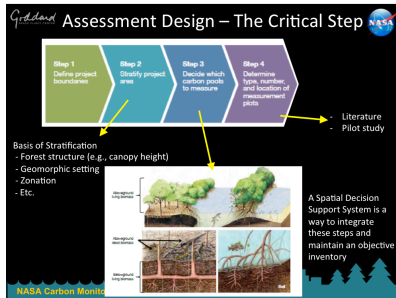
There are two basic types of sampling design

	Probability-based	Judgmental
Advantages	<ul style="list-style-type: none"> Provides ability to calculate uncertainty associated with estimates Provides reproducible results within uncertainty limits Provides ability to make statistical inferences Can handle decision error criteria 	<ul style="list-style-type: none"> Can be less expensive than probabilistic designs. Can be very efficient with knowledge of the site Easy to implement
Disadvantages	<ul style="list-style-type: none"> Random locations may be difficult to locate An optimal design depends on an accurate conceptual model 	<ul style="list-style-type: none"> Depends upon expert knowledge Cannot reliably evaluate precision of estimates Depends on personal judgment to interpret data relative to study objectives

U.S. DEPARTMENT OF AGRICULTURE
NATIONAL AGRICULTURAL LIBRARY

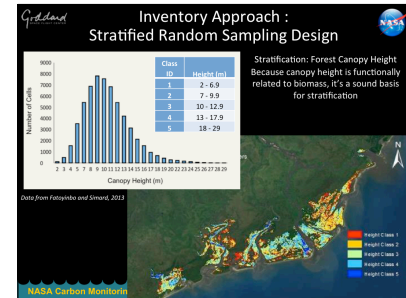


Objective sampling designs are fundamental to quantifying stocks within an area of interest; it also provides a rational basis for assessing uncertainties in the measurements. Subjective sampling designs are useful for characterization or pilot studies; but inappropriate for extrapolation beyond the investigation sites.



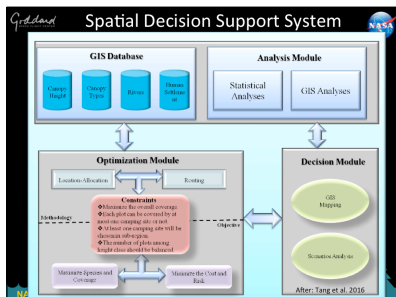
The objective inventory design requires the user to 1) define the project boundaries, 2) stratify the project area, 3) decide which carbon pools to measure, and 4) determine the number, type, and location of measurements.

49



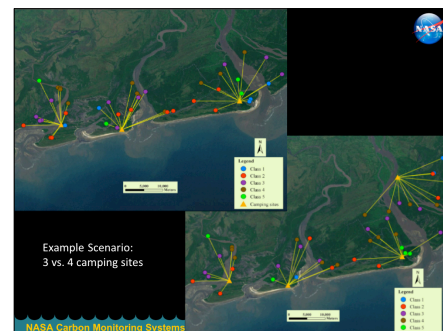
The remote sensing data can provide advanced information about an assessment area. We used mangrove extent and canopy height estimated using remote sensing data as the basis for stratification in the sampling design. Each height strata were determined to contain approximately equal areas.

50

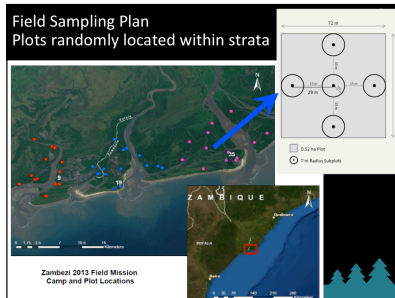


The Spatial Decision Support System was configured to enable the inclusion of operational constraints while objectively allocating sampling plots within the inventory area. First, we use empirical data from the pilot field mission and remote sensing data to allocate plots among the sample strata objectively. Then we prescribe the location of sample plots and camping sites based on logistical constraints while ensuring an objectivity. These constraints incorporated water access transport distance, and the location of villages.

51

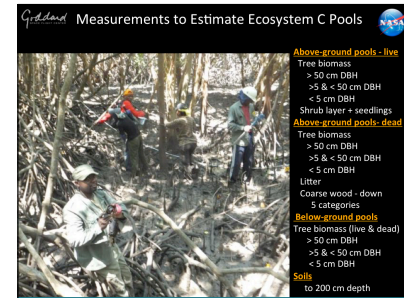


Here we show an example of the stratified plot locations and camping sites using a 3-camp and 4-camp scenario.



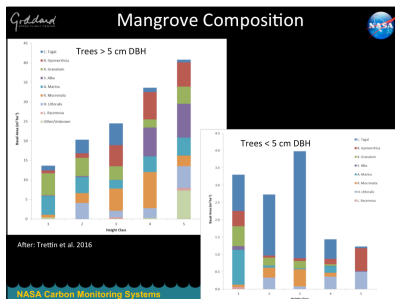
The Spatial Decision Support System provided the basis for objectively allocating field plots within the designated inventory area, which was the delta of the Zambezi River. At each sampling location a standardized protocol was implemented; the configuration of subplots within the inventory plot is shown in the top right. .

53



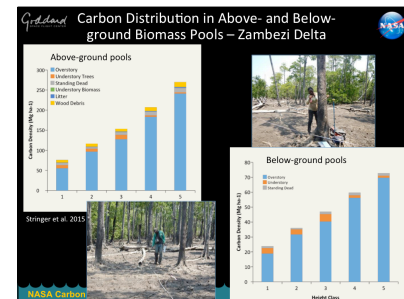
Field measurements included provisions to estimate total above- and below-ground biomass, and sampling soils to a depth of 200 cm.

54



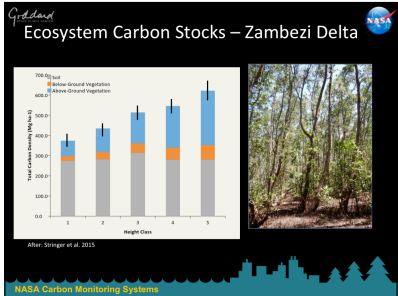
The inventory facilitates the assessment of the species composition within strata. Eight species of mangroves were encountered in the Zambezi. The distribution of species varied among height class strata and tree size class.

55

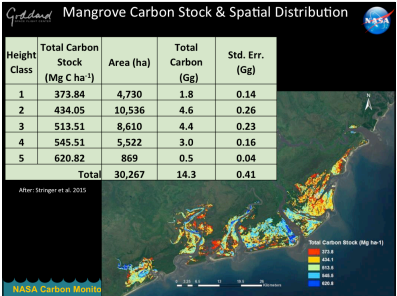


Trees (> 5 cm DBH) comprise the majority of above- (73-89%) and below-ground (79-96%) biomass.

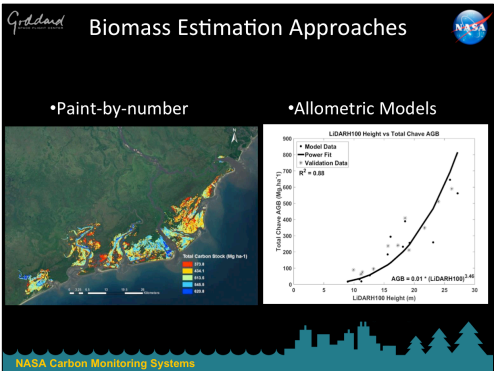
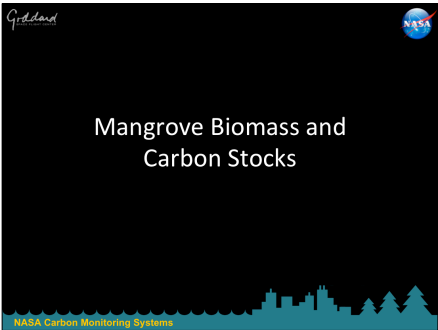
56

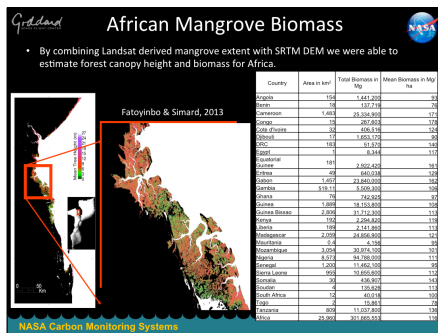


Total carbon densities range from 374-620 Mg C/ha, with the density increasing from height class 1 to 5. The soil component accounts for 45-73% of total density, and is the largest component of the ecosystem carbon pool. Soil carbon was similar among height class strata; hence, differences were due to biomass carbon. Above-ground biomass ranged from 20-34% of total stock, below-ground biomass ranged from 6-12%.



The inventory facilitates the calculation of the total carbon stock which is estimated as 14.3 Gt C., the 95% confidence interval is +/- .82 Gg. Accordingly, the 95% CI is 5.7% of the estimated mean (e.g. total). Well within IPCC guidelines. The use of canopy height strata facilitates displaying the distribution of carbon within the landscape.

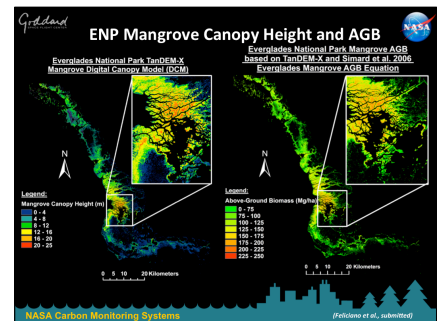




Applied Allometric Equations

Illustrated here is one of the earlier studies to use a combination of Landsat derived mangrove extent with SRTM DEM to estimate forest canopy height and biomass for mangroves in Africa. At that time, the SRTM data was only available at 90 m resolution globally. This data has been rereleased and is now available at 30 m globally. We are currently working on releasing global canopy height and global mangrove biomass datasets.

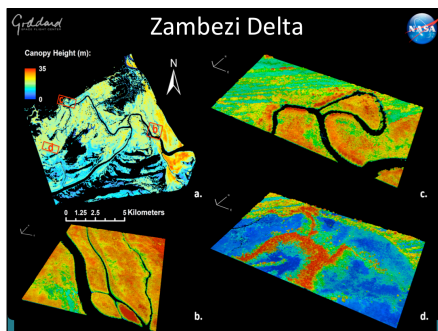
61



Applied Allometric Equations

Here we show an example of mangrove canopy height with TanDEM-X data in the Everglades National Park. In order to estimate biomass, we applied a global mangrove allometric equation (Simard et al. 2006). Mangroves canopy height ranges from 9 to 12 m. The AGB for Everglades National Park is 6.4×10^9 Kg, a little higher than the previous estimate 5.6×10^9 kg. Most of the AGB lies between 90 Mg/ha and 120 Mg/ha.

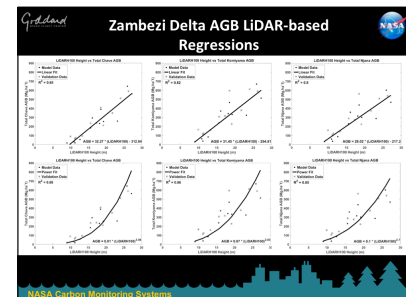
62



Zambezi Delta

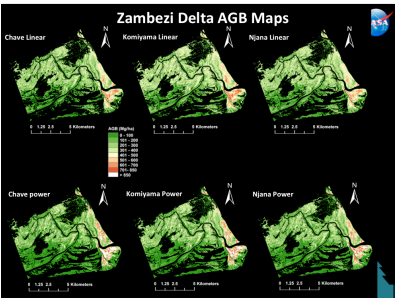
Zambezi River Delta is the first area where we started working, because there was an existing REDD readiness project with USFS, CIFOR and WWF. This was the first test for USFS of the height based stratification. This also allowed us to collect Lidar data over the Zambezi.

63



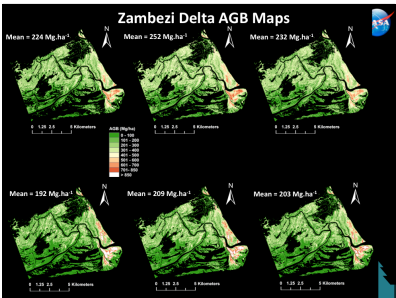
The availability of ALS and field data, enable us to create allometric regressions that can be used to predict AGB on mangrove forests. Here I'm just showing some examples of linear and power regressions created by comparing LiDAR H100 height with field-based AGB estimates from various mangrove allometric equations.

64



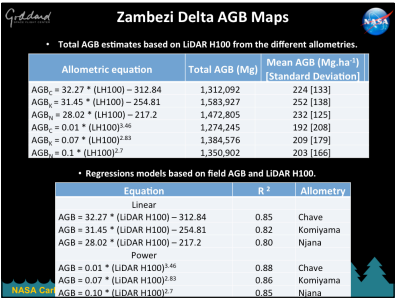
Zambezi River Delta Biomass Maps

Here we show the results of applying these regressions to ALS data. On the top row you can see the linear-based models and on the bottom row you can see the power law-based models. Results suggest that the power model is the best model.



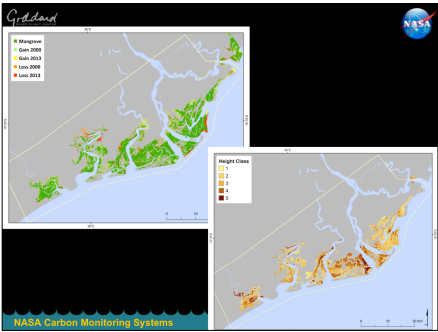
Zambezi River Delta Biomass Maps

Here we show the results of applying these regressions to ALS data. On the top row you can see the linear-based models and on the bottom row you can see the power law-based models. Results suggest that the power model is the best model.



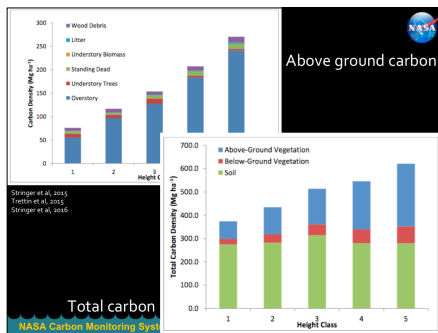
Zambezi River Delta Biomass Results

Here we show the allometric models, regression results and biomass statistics for the Zambezi River Delta region. LiDAR height was used to estimate biomass as it is the “gold-standard” and more easily available dataset for scientists.



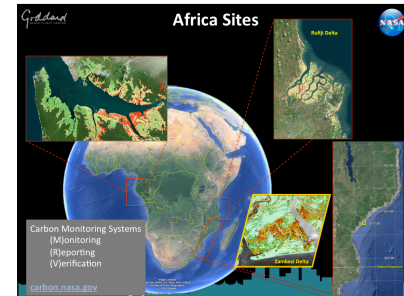
Combining Land Cover and Canopy Height

When we combine our land cover, land cover change, and canopy height models we can estimate carbon capture potential and carbon emissions. If we know the canopy height and mangrove extent we can estimate biomass at time 1. Remeasuring canopy height (and biomass) and mangrove extent at time 2 we can then estimate how fast mangrove biomass is being accumulated or released.



Total Carbon by Height Class

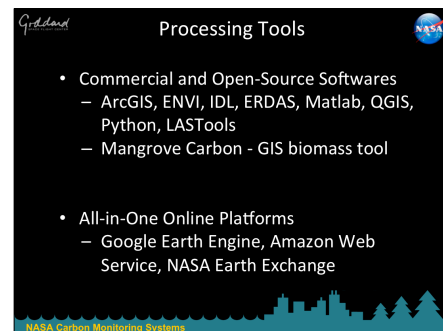
Combining the forest canopy height distribution from our digital canopy models and the field inventory data, biomass and carbon density can be determined for each height class. The top left figure shows the major aboveground components of forest biomass. These carbon values are determined directly from averaging the field inventory data for within each height class, using global/regional allometric equations. On the bottom right, the total carbon density values are plotted with each height class. The total density includes, the aboveground, belowground, and soil carbon.



Summary Slides

The approach that we have illustrated in this presentation has also been implemented in the Rufiji Delta (Tanzania) and Pongara National Park (Gabon). The results from these studies will be out soon, and data will be made available.

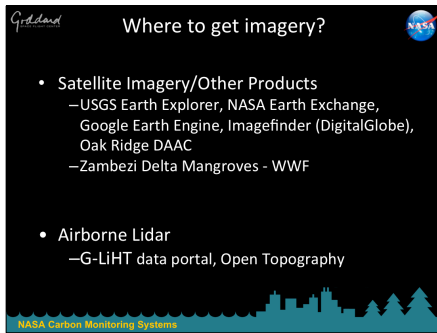
70



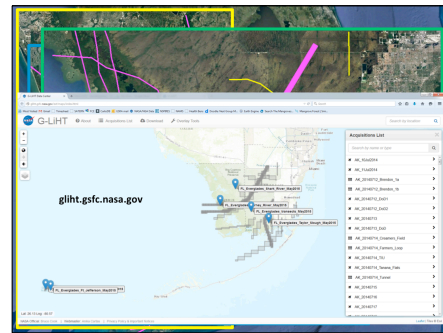
Useful Remote Sensing Image Processing Tools

There are many useful processing tools, some easier than others, to assist with the image processing. For optical and radar remote sensing data, ArcGIS, QGIS, ENVI, IDL, and ERDAS Imagine can be useful software to process images that you have downloaded. Online platforms such as Google Earth Engine, Amazon Web Services, and NASA Earth Exchange are useful applications where you have access to a large library of satellite imagery and spatial datasets and how the power to develop your own programming to process imagery.

LASTools is used to process raw LiDAR data and convert it to canopy height and forest metric products. Please refer to <https://rapidlasso.com/category/tutorials/> to download

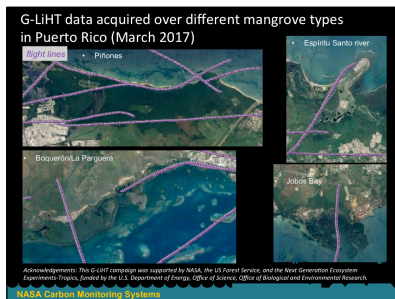


Useful Remote Sensing Image Archive



Airborne Lidar in Mangroves

Airborne lidar has been collected over a number of mangrove forests. Here we will highlight openly available airborne lidar data that was collected recently using NASA Goddard's Lidar, Hyperspectral, and Thermal Imager (G-LiHT). This is a state-of-the-art imager that combines three types of land imaging sensors that are all collected simultaneously. A few months ago, G-LiHT has had a new sensor added that can also measure fluorescence. A few months ago, G-LiHT collected data over the coastal wetlands of Florida Everglades and Puerto Rico.



G-LiHT in Puerto Rico

A recent effort by the US Department of Energy, NASA, and the US Forest Service collected G-LiHT data across Puerto Rico, including in different mangrove types, as shown in the figures. This data will be publicly available after processing and quality control.



MangroveScience.org

Our website has information about our past and ongoing projects. There is information about remote sensing techniques, links to different citations and resources, and has a data portal to connect you to available or soon-to-be available remote sensing data products.






References

1. Lagomasino, D., T. Fatoyinbo, S.K. Lee, E.A. Feliciano, C.C. Trettin, M. Simard, 2016. A comparison of mangrove canopy height using multiple independent measurements from land, air, and space. *Remote Sensing* 8, 327; doi: 10.3390/rs8040327.
2. Shapiro, A.C., C.C. Trettin, H. Küchly, S. Alavinasanah, and S. Bandiera, 2015. The mangroves of the Zambezi Delta from 1995 to 2013 increase in extent observed via satellite. *Remote Sens.* 7, 16504-16518. doi:10.3390/rs70x000x
3. Stringer, C.E., C.C. Trettin, S.J. Zarnoch, W. Tang, 2015. Carbon stocks of mangroves within the Zambezi River Delta, Mozambique. *For. Ecol.Mgt.* 354:139-148
4. Stringer, C.E., C.C. Trettin, S.J. Zarnoch, 2016. Soil properties in contrasting geomorphic settings within the Zambezi River Delta, Mozambique.
5. Tang, W., W. Fang, J. Deng, M. Jia, H. Zuo, C.E. Stringer, C.C. Trettin, 2016. A cyber-enabled spatial decision support system to inventory mangroves in Mozambique: Coupling scientific workflows and cloud computing
6. Trettin, C.C., C.E. Stringer, S. Zarnoch, 2016. Composition, biomass, and structure of mangroves within the Zambezi River Delta. *Wetlands Ecology Management*. doi: 10.1007/s11273-015-9465-8.




NASA Carbon Monitoring Systems

Acknowledgements

Bandiera, Salomão; Dept. of Biology, Univ. Eduardo Mondlane.
 Dai, Zhaohua; USDA Forest Service.
 Fatoyinbo, Temilola; Goddard Space Center, NASA.
 Feliciano, Emanuelle; Goddard Space Center, NASA.
 Lagomasino, David; Goddard Space Center, NASA.
 Lee, Seung Kuk, Goddard Space Center, NASA.
 Mabunda, Rito, WWF-Mozambique.
 Macamo, Celia, Dept. of Biology, Univ. Eduardo Mondlane.
 Nicolau, Denise; WWF-Mozambique
 Shapiro, Aurélie; WWF – Germany.
 Simard, Marc; Jet Propulsion Laboratory.
 Stringer, Christina; USDA Forest Service.
 Trettin, Carl; USDA Forest Service.
 Zarnoch, Stanley; USDA Forest Service
 Thomas, Nathan; Jet Propulsion Laboratory



NASA Carbon Monitoring Systems




Acknowledgements
















NASA Carbon Monitoring Systems